Research Article | Vol. 29, No. 9 / 26 April 2021 / Optics Express 13669
Optics EXPRESS

Micro two-dimensional slit-array for super resolution beyond pixel Nyquist limits in grating spectrometers

MINGBO CHI,[1] XINXIN HAN,[1,2] YANG XU,[1] HUAMING XING,[1] YONGSHUN LIU,[1] AND YIHUI WU[1,*]

[1] State Key Laboratory of Applied Optics, Changchun Institute of Optics, Fine Mechanics and Physics, Chinese Academy of Sciences, Changchun 130033, China
[2] University of Chinese Academy of Sciences, Beijing 100039, China
[*] yihuiwu@ciomp.ac.cn

Abstract: This paper presents a new micro 2-D slit-array device for spectral resolution enhancement in grating spectrometers. The 2-D slit-array is encoded in Hadamard matrix and the device is fabricated based on the micro-electromechanical system (MEMS) technology. By just using this 2-D slit-array to replace the single slit in the conventional grating spectrometer, real-time super spectral resolution detection beyond the pixel Nyquist limit, which is determined by the size of the detector pixel, can be realized. Furthermore, no other configuration of the spectrometer is changed, no movable parts are used, and the spectral range and instrument size remain almost unchanged while the resolution is improved. A series of experimental verifications for the feasibility of this design are included in this work.

1. Introduction

Grating dispersion is typically used in spectral detection and it is useful for the full optical region from UV to the infrared. The performance of spectrometer is mainly determined by the spectral resolution in relation with spectral range, and the signal-to-noise ratio (SNR) [1]. The spectral resolution of grating spectrometer is limited by the grating dispersion value, width of slit and detector pixel size. The strongest of these limits determines the achievable resolution. It is usually said that the spectral resolution of grating spectrometer may be improved by using larger dispersion value, narrower slit or smaller detector pixel size. However, larger dispersion value means larger grating groove density or larger dispersion length. Grating groove density is limited by current manufacture technology, and large dispersion distance conflicts with miniaturization of the instrument, which is sought after for a wide range of applications [2–5]. On the other hand, large dispersion value will cause the spectral range to reduce when using a proper multi-channel detector. Narrowing the entrance slit width to upgrade the spectral resolution is the simplest option regardless of increase in size and cost, but this will lead to the decrease of SNR. In previous studies, the introduction of multi-slit in the grating spectrometer is used to improve its throughput [6–8], although the improvement effect is usually not as good as that obtained by the Fourier transform infrared spectrometer through the Jacquinot or throughput advantage [7–9].The conventional multi-slit can't solve the limitation of detector pixel size on the system spectral resolution so its resolution limit is the same as that of a conventional single slit grating spectrometer. The design of the entrance slit width is usually determined by the detector pixel size according to the Nyquist sampling theorem [10] because the pixel size of detector has a certain limitation (several microns to a few tens of micron) in terms of sensitivity and manufacture technology which leads to sampling insufficiency in the practical application [11]. So it is difficult to just improve the resolution, especially to break the Nyquist limits determined by the detector

#420552 https://doi.org/10.1364/OE.420552
Journal © 2021 Received 22 Jan 2021; revised 8 Apr 2021; accepted 8 Apr 2021; published 21 Apr 2021

Optics EXPRESS

pixel size, without worsening the other performance aspects, especially spectral range and the signal-to-noise ratio, and without essentially increasing the size of the grating spectrometer.

By eliminating the restriction of the slit width with signal processing methods such as deconvolution method [12], the instrument's resolution can be enhanced without physically changing its configuration but prior knowledge about the instrument or special signal processing methods is needed. Moreover, the best resolution obtained by this way is usually determined by the pixel Nyquist limit [13]. The detector pixel size can be virtually decreased by subpixel methods [14] and the reduced pixel size has to be considered for increasing the resolution of the instrument. Super resolution spectrum can be extracted from a set of differently sampled spectra to exceed the pixel Nyquist limits. Previously, such a set of spectra was generated by shifting the detector or the entrance slit of the instrument [15,16]. The scanning of these spectral frames will increase the acquisition time which leads to the trade-off between the spatial and temporal resolution [17], and the introduction of movable part will reduce the robustness and compactness of the spectrometer. Moiré effect was used to realize super spectral resolution beyond the Nyquist limits in the grating spectrometer, which uses a pair of periodic slits with slightly different periods in the entrance and exit plane of the instrument, respectively [18,19]. In this method, the observable spectral range is determined by the period of the slits, and it is suitable for applications with limited observation spectral range.

In this report, we propose a new micro 2-D slit-array device to achieve super resolution beyond the pixel Nyquist limits in grating spectrometer. This 2-D slit-array is encoded in Hadamard S-matrix [20] and used to replace the long slit in conventional grating spectrometer. Through this static slit-array functioning together with a 2-D detector, a set of different spectra with different sub-pixel displacements in the dispersion direction are generated simultaneously after the decoding process. Super resolution spectrum can be obtained by the implementation of conventional sub-pixel reconstruction method [15,21], and significant SNR compensation can be achieved by Hadamard Transform, while the spectral detection range of this instrument remains almost unchanged. Moreover, no movable part is used in this device and it can realize real-time spectral detection.

2. 2-D slit-array for super-resolution detection

As Fourier transform spectroscopy which uses an interferometer to obtain Fellgett and Jacquinot advantage, the grating spectrometer can obtain similar optical multiplexing advantage to improve the instrument performance by introducing encoding devices such as 2-D slit-array to realize Hadamard transform. As shown in Fig. 1, an encoding mask with 2-D slit-array is used to replace the traditional single slit to implement the multichannel spectral detection together with a 2-D detector. The slit-array is encoded in an N*N binary matrix, which usually utilizes a Hadamard matrix so that the decoded spectrum of each channel has better SNR. In terms of SNR according to Hadamard transform theory, Hadamard S-matrices make the best masks when only entries 1 and 0 can be used in the scheme for multiplexing measurement shown in Fig. 1 [8,20].

In the Hadmard encoding process shown in Fig. 1, slits in the same column of the 2-D slit-array belong to the same spectral channel and produce same spectral distributions because they have the same location in the dispersion direction. The spectral signals produced by the slits in the same row are sampled by the same pixel of the detector, which can be seen as a form of multiplexing. For this pixel, it collects spectral signal from different channels to realize a compound measurement. In each compound measurement, code 1 in the encoding matrix means that the corresponding spectral channel is included in the measurement, and code 0 means not. Then the pixels in the same column of the detector collect all different compound measurement results, which are denoted by column vector Y. If S_k is used to denote the spectral intensity of the kth channel on this column of pixels, H is used to denote the encoding matrix, and n_d is used to

Optics EXPRESS

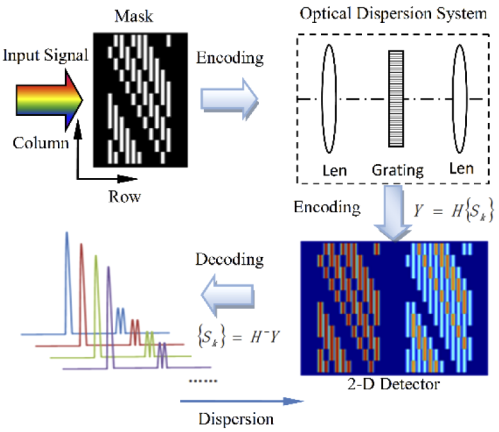

Fig. 1. Multi-channel detection based on Hadamard Transform in grating spectrometer

denote the random noise from the detector, the encoding process can be descripted as

$$Y = H\{S_k\} + n_d. \tag{1}$$

A 2-D imaging detector samples the encoding data Y, translates it into digital signal and then transmits it to the computer for decoding process. By performing the inverse Hadamard transform as shown in Eq. (2), we can get the spectrum of each spectral channel and the SNR of each decoded spectrum is increased accordingly [22].

$$H^{-}Y = \{S_k\} + H^{-}n_d. \tag{2}$$

After the above processing for each column of data of the 2-D detector, multi-channel spectral detection can be obtained through only one data acquisition.

The 2-D slit-array and the grating dispersion system function together to implement the encoding process of the Hadamard transform. The light signals of all the spectral channels come from the same light source. However, as shown in Fig. 1, there is a shift between the decoded spectra of these spectral channels because of the distance between the corresponding columns of slits in the dispersion direction. The shift of the decoded spectra on the detector is proportional to the column pitch between the corresponding spectral channels which is denoted as c as shown in Fig. 2. If the shift between the decoded spectra of corresponding channels corresponds to integer pixels, the decoded spectra of these channels are the same after shift calibration. However, if the shift of the decoded spectrum is not integer pixels and has sub-pixel components, the decoded spectrum of the corresponding channel contains different spectral information of the light source. Based on these characteristics of Hadamard multi-channel detection, we propose a new design of the static 2-D slit-array to achieve super resolution beyond pixel Nyquist limits for a grating spectrometer by the combination of Hadamard transform and sub-pixel method. Figure 2 shows the schematic configuration of the instrument and the conceptual procedure of the resolution enhancement. The slit column pitch c is the key parameter of this new 2-D slit-array design, and its calculation method based on a Czerny-Turner grating spectrometer [23] is expressed as

$$c = \frac{(\mathrm{J} + 1/\mathrm{n})pf_1\sqrt{1 - (\mathrm{m}\lambda/\mathrm{d} - \sin\alpha)^2}}{f_2\cos\alpha}, \tag{3}$$

where f_1 and f_2 is the focus of the collimation mirror and condensing mirror respectively, d is the grating groove spacing, m is the diffraction order, λ is the wavelength of light signal, α is

Optics EXPRESS

incident angle of the grating, p is the detector pixel pitch, J is an integer corresponding to the integer pixel part of the shift, and n is the designed resolution gain.

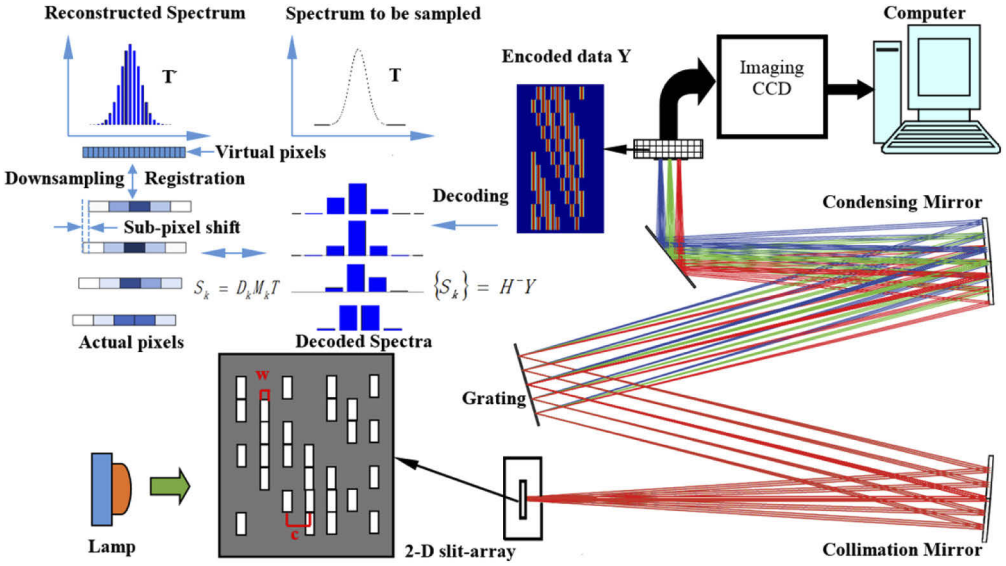

Fig. 2. Schematic of the principle of super resolution detection based on 2-D slit-array

By accurately setting the slit column pitch c as shown in Fig. 2, the sub-pixel shift between the decoded spectra of different channels can be generated. With 1/n pixel shift, the resolution of the spectrometer can be improved by n times in theory [24]. In other words, having acquired n different decoded spectra with low resolution at the same time, each shifted by 1/n pixel, the profile of the spectrum to be sampled can be suitably reconstructed with an n times improved resolution as shown in Fig. 2. In fact, the use of this 2-D slit-array is equivalent to constructing virtual smaller pixels whose size are equal to the sub-pixel shift, thereby improving the instrument's actual sampling rate and then realizing super spectral resolution beyond Nyquist limits. However, the actual resolution of grating spectrometer is affected by both the sub-slit width and detector pixel size. Corresponding to 2 virtual smaller pixels according to Nyquist sampling theorem [10], the sub-slit width denoted as w is calculated as

$$w = 2\frac{p}{n}\frac{f_1\sqrt{1-(m\lambda/d-\sin\alpha)^2}}{f_2\cos\alpha}. \tag{4}$$

According to the above calculation, the design of the encoding mask is completed. By installing the mask into the system as shown in Fig. 2, multi-channel and different spectral detection can be realized through a single measurement. If T is the spectral signal to be sampled, the spectrum of kth channel denoted as S_k can be described as

$$S_k = D_k M_k T, \tag{5}$$

where M_k is the sub-pixel shift operator, and D_k is the downsample operator. Through this model, the relationship between the decoded spectrum of each channel sampled by actual pixels and the signal to be measured can be established. After obtaining the series of decoded spectrum with different sub-pixel shifts, the super resolution spectral signal can be reconstructed according to the sub-pixel method [15,21]. The first step of super-resolution reconstruction is the registration between different decoded spectra, which is to construct the sub-pixel shift matrix M according to

Optics EXPRESS

the sub-pixel shift between them. The sub-pixel shift between the decoded spectra is determined by the encoding mask, so based on Eq. (3), the sub-pixel shift matrix M can also be determined accordingly. The actually obtained super-resolution spectrum T′ is also a discrete spectrum, which is equivalent to sampling the spectral signal T using virtual pixels with a much smaller size which is equal to the sub-pixel shift as shown in Fig. 2. The size of the virtual pixel is one-nth of the actual pixel size, then the downsampling matrix D can be constructed based on this assumption. However, it also means that the unknown quantities need to be solved in the reconstruction process is n times the amount of the spectral data in low resolution spectra. According to the sub-pixel method in image processing [24,25], the multi-frame super resolution reconstruction can be formulated as an optimization problem with a regularizer for the penalty shown as

$$T' = \arg\min_{T} \left\{ \sum_{k=1}^{n} ||D_k M_k T - S_k||_2^2 + \lambda\gamma(T) \right\}, \tag{6}$$

where λγ(T) is the regularization term and T′ is reconstructed spectrum with super resolution beyond pixel Nyquist limits.

3. Experiment verification

3.1. Experimental setup

The resolution enhancement effect of the designed 2-D slit-array is experimentally verified based on a grating spectrometer built in our lab as shown in Fig. 3(a). The structure of the spectrometer is as same as a traditional Czerny-Turner type spectrometer except the entrance slit, which is replaced by the 2-D slit-array as shown in Fig. 3(b). This 2-D slit-array is encoded in Hadamard S matrix and etched on silicon wafer based on MEMS technology. The wafer thickness is 280 microns and dry etching is used in the fabrication process. In order to obtain better machining accuracy and slit edge roughness by reducing the etching depth of 2-D slit-array structure, two etchings were carried out on both sides of the silicon wafer respectively. The thickness of the area for 2-D slit-array processing is reduced to about 50 microns by the first etching. Then the 2-D slit-array structure is etched from the other side. An Hg lamp is chosen as the light source for its discrete spectrum with sharp peaks. The measured light is guided to the 2-D slit-array through a fiber and a collimator for uniform illumination. After being encoded by the 2-D slit-array, the incident light is dispersed by the grating dispersion system, which is composed of two 60mm focal length concave mirrors, and a 600 line/mm grating. Then the encoded data is collected by an imaging CCD detector with a 14μm pixel size (Hamamatsu) and then transmitted to the computer for decoding and super-resolution reconstruction process.

3.2. Experimental results on resolution enhancement

In order to verify the feasibility of the micro 2-D slit-array device proposed in this paper, we conducted a series of experiments to perform super-resolution observations on the 3 spectral lines of the mercury lamp in 540-590nm band. To highlight the effect of pixel pitch on the spectral resolution, we use the detector's binning mode, which is to synthesize multiple adjacent pixels into one pixel, thereby constructing 56μm pixels and 28μm pixel respectively for comparative experiments. As shown in Fig. 4(a), we fabricated an encoding mask with a 2-D slit-array encoded in Hadamard S matrix of order 7. The width of the sub-slit in the 2-D slit-array is designed to be 27μm, so that the spectral resolution of the spectrometer is mainly limited by the detector pixel according to Eq. (4). The slits in the same column belong to the same spectral channel. The 7 spectral channels of this 2-D slit-array are divided into two groups, group A contains 3 channels and group B contains 4 channels respectively. In each group, the column spacing of two adjacent columns of slits corresponds to one detector pixel, so that the decoded spectra of each channel in the same group are uniformly sampled and have the same spectral distribution after performing

Optics EXPRESS

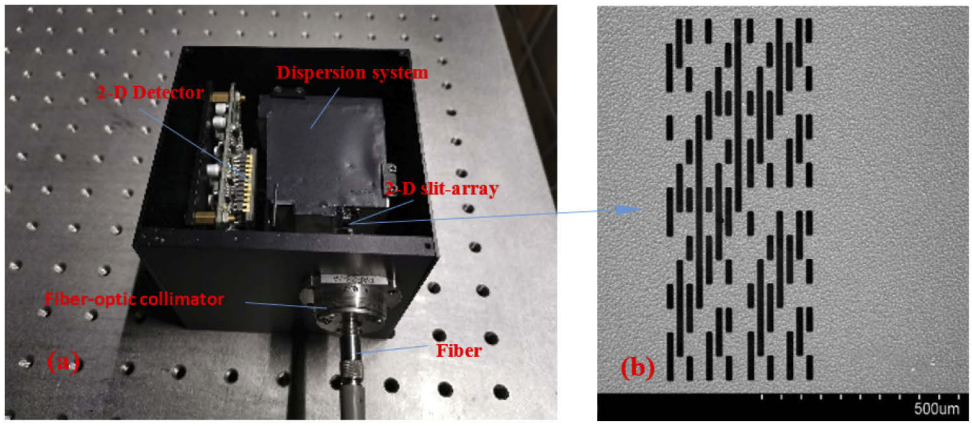

Fig. 3. (a) Photograph of experimental setup, (b) the structure of the 2-D slit array observed under the scanning electron microscope.

the integer pixel shift calibration. The average of these corrected spectra in the same group was taken as the decoded spectrum of this group. Moreover, the distance between channel 3 of group A and channel 4 of group B corresponds to 1.5 detector pixels, so that there is a half-pixel offset between the decoded spectra of the two groups of spectral channels.

After the light signal from the Hg lamp is modulated by the designed 2-D slit-array, the encoding data collected by the detector with 56μm pixels is shown in Fig. 4(b) and the decoded spectra of the two groups are shown in Fig. 4(c) and (d) respectively. As we can see from the encoded data shown in Fig. 4(b) and the two decoded spectra, the spectral channels in different groups carry different spectral information because of the sub-pixel shift. Influenced by large pixel pitch, the two decoded spectra have low resolution, so the two spectral peaks at 577nm and 579nm of the Hg lamp can't be distinguished and appear as one spectral line. By comparing spectral lines at 577nm-579nm band in the decoded spectra shown in Fig. 4(c) and Fig. 4(d), there are significant differences between the decoded spectra of the two groups of spectral channels caused by the sub-pixel shift. Making use of the two different decoded spectra to perform the super-resolution reconstruction, the reconstructed spectrum is shown in Fig. 4(f).

For comparison, we also fabricated a long single slit with a width of 27μm, which is the same as the width of the sub-slit in the slit-array. The spectrum shown in Fig. 4(e) is detected using the long single slit and the detector with 56μm pixel size. As shown in Figs. 4(c), (d) and (e), the FWHM (full width at half maxima) of the spectral peak at 546nm are all about 3.2nm. That means the decoded spectra using Hadamard 2-D slit-array have nearly the same spectral resolution with the one directly detected using the traditional long single slit when the other configurations in the spectrometer remain unchanged. The FWHM of the super-resolution reconstructed spectral peak at 546nm shown in Fig. 4(f) is only about 1.6nm, which is as same as the spectrum detected using the long single slit and detector with 28μm pixel pitch as shown in Fig. 4(g). Both in the super-resolution reconstructed spectrum using the 2-D slit-array and the spectrum detected with smaller size pixel detector, the spectral peaks at 577nm and 579nm can be well distinguished. By comparing the reconstructed spectrum shown in Fig. 4(f) and the spectrum shown in Fig. 4(e) which are both detected using the detector with 56μm pixel, we can find that replacing the traditional slit with the 2-D slit-array in the spectrometer significantly improves the system resolution. By comparing the reconstructed spectrum shown in Fig. 4(f) and the spectrum shown in Fig. 4(g) which have nearly the same resolution, we can find that the resolution enhancement effect obtained by the 2-D slit-array is almost the same as the resolution enhancement effect obtained by reducing the pixel size of detector and the designed 2-D slit-array

Optics EXPRESS

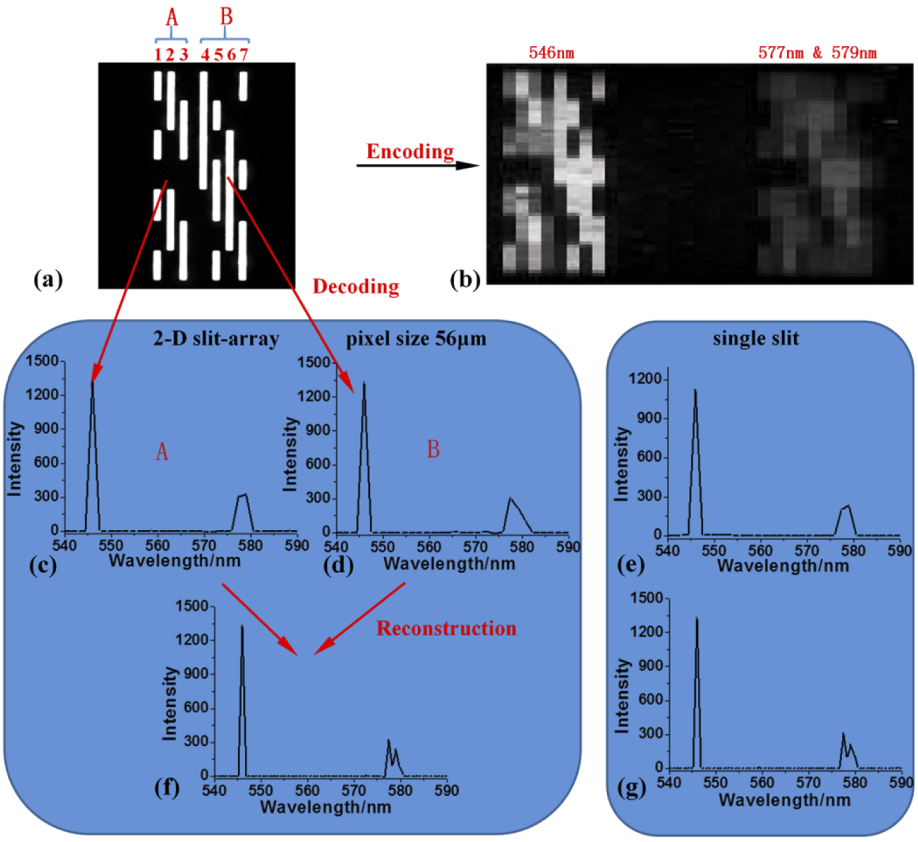

Fig. 4. Experimental results for the super resolution reconstruction using a detector with 56μm pixel size. (a) Image of the 2-D slit-array encoded in Hadamard S matrix of order 7 observed under optical microscope. (b) The encoded data of 546 nm, 577 nm, 579 nm spectral lines of Hg lamp on the detector with 56μm pixel size. (c) The decoded spectrum of spectral channels in group A. (d) The decoded spectrum of spectral channels in group B. (e) The spectrum detected using the single slit and detector with 56μm pixel size (f) The super-resolution reconstructed spectrum using the 2 spectra shown in c and d. (g) The spectrum detected using the single slit and the detector with 28μm pixel size.

can break through the pixel Nyquist limit which is the limitation of the detector pixel size on the system resolution.

Therefore, the experimental comparison shows that the resolution of the spectrometer has been increased by a factor of about 2 after the super-resolution reconstruction with 0.5 sub-pixel shift based on the specially designed 2-D slit-array. Comparing the reconstructed spectrum with the decoded spectra, the spectral detection range remains almost unchanged with the increase of the spectral resolution. Moreover, only one data collection is needed in the super spectral resolution detection process and no movable parts is used. So the new 2-D slit-array proposed in this paper can realize real-time super-resolution spectral detection while the spectral detection range and the other configuration of the instrument remains almost unchanged.

To further eliminate the effect of slit width on resolution, we fabricated three different kinds of entrance slits, which are used with the same 2-D CCD detector with 14μm pixel pitch to implement spectral detection. There is a 2-D slit-array encoded in 15-order Hadamard S matrix as shown in Fig. 3(b). The width of the sub-slit in the array is 14μm according to Eq. (4). The

Optics EXPRESS

15 spectral channels on this mask are also divided into two groups, which have a relative shift of half a pixel. The super-resolution beyond Nyquist limit can be obtained after reconstruction process. For the other two slits for comparative experiments, they are long single slits with width of 14μm and 27μm, respectively. The super resolution reconstructed spectrum using the 2-D slit-array is shown in Fig. 5 as well as the measured spectra using the single slits with different width. As shown in Fig. 5, the FWHM of the reconstructed spectrum using 2-D slit-array at 546nm, 577nm and 579nm is about 0.6nm, while the FWHM of the spectra using long single slit with width of 14μm and 27μm are both about 0.8nm. Thus with the designed 2-D slit-array shown in this report, the spectral resolution of the spectrometer has been significantly improved compared with spectrum detected with the traditional single slits.

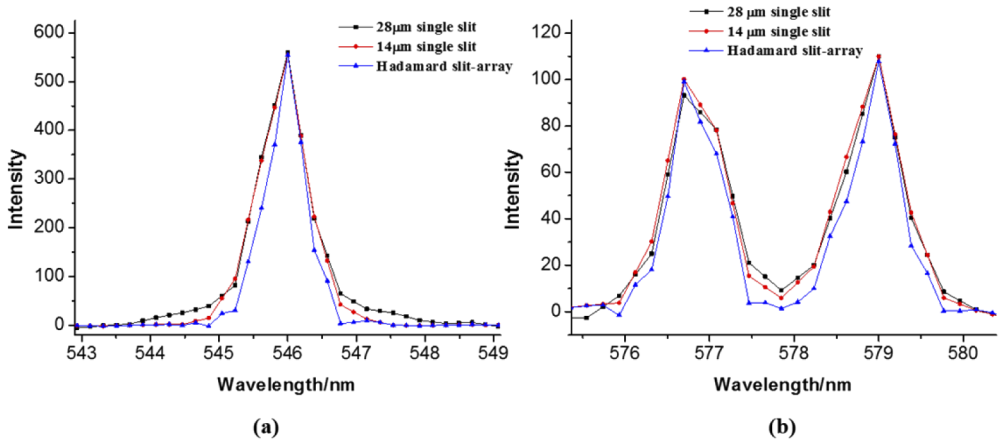

Fig. 5. Comparison of spectra measured using the same detector and three different mask. (a) 546 nm spectral line of Hg lamp. (b) 577 nm and 579 nm spectral lines of Hg lamp.

3.3. Experimental results on SNR enhancement

To verify the throughput and SNR compensation brought by the 2-D slit-array in the process of super spectral resolution detection, we fabricated a new mask as shown in Fig. 6. The mask is divided into 2 parts, one contains a 2-D slit-array encoded in Hadamard S matrix of order 15, and the other contains 15 shifted single slits arranged in a diagonal matrix. The two kinds of incident slits have the same size sub-slit. The sub-slits in the corresponding column in the two incident slits have the same location along the diffusion direction so that these two kinds of incident slits have the same spectral channel arrangement and can achieve the same sub-pixel super-resolution detection. The reconstructed spectra with super-resolution obtained using these two kinds of slits have nearly the same FWHM. The difference lies in that there is only one slit in each row of shifted slits arranged in diagonal matrix, and the spectrum of each single sub-slit or each channel can be obtained without decoding. However, for the case of 2-D slit-array encoded in Hadamard matrix, the spectrum of each channel has an improved SNR after the decoding process compared with the spectrum directly generated by the sub-slit, thereby improving the SNR of the spectrum with super resolution after subsequent reconstruction process.

We installed the above mask in the experimental system as shown in Fig. 3(a) and used these two kinds of slits for super-resolution spectral detection, so as to conduct a signal-to-noise ratio comparison experiment under the same incident light signal to exclude the influence of light source intensity fluctuations on the experimental results. We performed 40 measurements and recorded the peak intensity values of the reconstructed spectra at 546, 577, and 579nm,

Optics EXPRESS

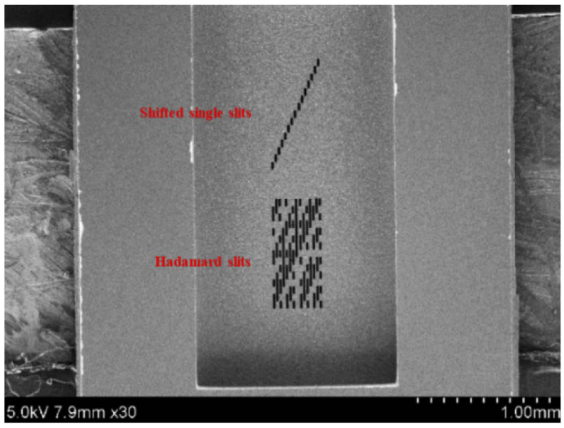

Fig. 6. Encoding mask with shifted single slit and Hadamard 2-D slit-array.

respectively. The SNR of each spectral peak intensity is calculated as

$$SNR = \frac{\bar{X}}{\sigma}, \tag{7}$$

where $\overline{X}$ is the mean value of the measured corresponding spectral peak intensities, and σ is the root mean square of these measured intensities. According to the calculation results, the SNR at 546nm, 577nm, and 579nm of the reconstructed spectra obtained by using the 2-D slit-array is improved by 1.31 times, 1.92 times, and 1.85 times, respectively, compared with the reconstructed spectra using the diagonal slits, while the theoretical SNR enhancement of 15^{th} order Hadmard 2-D slit-array is approximately 2 times [20].

The SNR gain from Hadamard transform, known as Fellgett's advantage, is usually based on the promise that only the signal-independent noise such as detector noise is considered. However, in actual experiments, the presence of signal-dependent noises such as photon shot noise will reduce the Fellgett's advantage. Therefore, the measured values for the Fellgett's advantage in the above experiment are all smaller than expected. Moreover, the stronger the signal, the greater the influence of the photon shot noises, and the less Fellgett's advantage can be obtained. The intensity of Hg-lamp at 546nm is stronger than the intensities at 577nm and 579nm, so the measured signal-to-noise ratio gain at 546nm is smaller than the others. The above experiment shows that the 2-D slit-array proposed in this paper can achieve SNR compensation while realizing super-resolution spectral detection of weak signals, which is of great significance to balance the contradiction between high resolution and high SNR in grating spectrometers.

4. Discussion

The feasibility of the micro 2-D slit-array for super resolution beyond Nyquist limits in grating spectrometer has been verified through comparative experiments described in Part 3.2. In a Czerny-Turner type grating spectrometer, the spectral bandwidth on a single pixel or the dispersive conversion rate can be calculated as shown in Eq. (8), which can be derived from the grating equation [26]. Here, p is the detector pixel pitch, d is grating groove spacing, m is the dispersion order, f_2 is the focal length of the condensing mirror, and β is the dispersion angle.

$$w = \frac{d\lambda}{dl}p = \frac{d\cos\beta}{mf_2}p. \tag{8}$$

In the experimental setup in this paper, the spectral bandwidth on single pixel at 546nm is about 0.4nm according to theoretical calculation based on Eq. (8), when the actual detector

Optics EXPRESS

pixel pitch is 14μm. So the Nyquist limit of this spectrometer when using single slit should be about 0.8nm. It is also found that in the experimental setup proposed above, when the single slit is used, the reduction of the slit width from 27μm to 14μm will not substantially increase the resolution of the spectral system, and the FWHM of the two detected spectrum are all around 0.8nm which is determined by the Nyquist limits. However, just by replacing the single slit with the proposed 2-D slit-array, and without changing any other configuration in the experimental setup, the FWHM of the reconstructed spectrum is decreased to about 0.6nm, which breaks the Nyquist limit of 0.8nm.

It can be proved by comparative experiment shown in Fig. 4 that the introduction of 2-D slit-array in grating spectrometer actually constructs virtual smaller pixels whose size is equivalent to the sub-pixel shift in the 2-D slit-array, thereby improving the instrument's actual sampling rate and then realizing super spectral resolution beyond Nyquist limits. The reconstructed spectrum can be regarded as obtained by the spectrometer which uses a detector with virtual small pixels. According to Eq. (8), the focal length of the condensing mirror can be reduced with the decrease of pixel size p, while the spectral bandwidth on single pixel which determines the resolution of the spectrometer remains unchanged. Reducing the focal length of the mirror without sacrificing the resolution is helpful for the reduction of the size of the grating spectrometer, thereby contributing to the miniaturization of the instrument. Moreover, there are no movable parts needed in this instrument. The elimination of movable parts helps to improve the compactness of the spectrometer, which is of great significance for both dispersive spectrometer and Fourier transform spectrometer [27].

When taking the FWHM as the measure standard, the spectral resolution enhancement after reconstruction is lower than the theoretically expected 2 times gain in the comparative experiments as shown in Fig. 5. In the proposed dispersion system, the focal length of collimating mirror is approximately the same as the one of the condensing mirror, and the magnification in the direction perpendicular to the dispersion direction is about 1. However, in the dispersion direction, the incidence angles of the two points (A and B as shown in Fig. 7(a)) on the two edges of the slit with respect to the grating are slightly different. Due to the dispersion of the grating, the distance between the corresponding points (A′ and B′ as shown in Fig. 7(b)) on the image plane will be widened, which will be also caused by the optical aberration, especially coma. We measured the width of the sub-slit of the 2-D slit-array shown in Fig. 6(a) under a microscope with large depth of field (Keyence), and the measured width is about 15μm as shown in Fig. 7(a). The fabrication error is about 1μm. ZEMAX software was used to simulate and calculate the center distance of the two spots on the imaging plane of the dispersion system. The simulated spot diagrams which correspond to 2 points with 15μm apart on the object plane in the dispersion direction are shown in Fig. 7(b), and the calculated width of the image of the sub-slit in the dispersion direction is about 18μm. Taking into account factors such as assembling and adjustment errors in experiments, the actual width may be wider. With the 0.5 pixel shift generated by the 2-D slit-array as shown in Fig. 3(b), the pitch of the virtual small pixel should be about 7μm, which means that the image of the sub-slit roughly corresponds to about 3 virtual pixels. According to Eq. (8), the dispersion conversion rate of this system is about 0.4nm/14μm, then the spectral bandwidth on single virtual pixel should be about 0.2nm. So the actual FWHM of the reconstructed spectrum is about 0.6nm, which is consistent with the experimental result.

Moreover, by improving fabrication accuracy to obtain even smaller sub-pixel shift, such as one-quarter, one-eighth, etc., we can accordingly achieve four times, eight times, and even higher resolution enhancement in theory. But in fact, we also need to consider the influence of the dispersion system on the FWHM of the reconstructed spectrum, reduce the width of sub-slit according to Eq. (4), improve the fabrication accuracy, optimize the optical system for aberration correction, and use deconvolution methods to process reconstructed signal, so that the actual resolution obtained is close to the theoretical value.

Optics EXPRESS

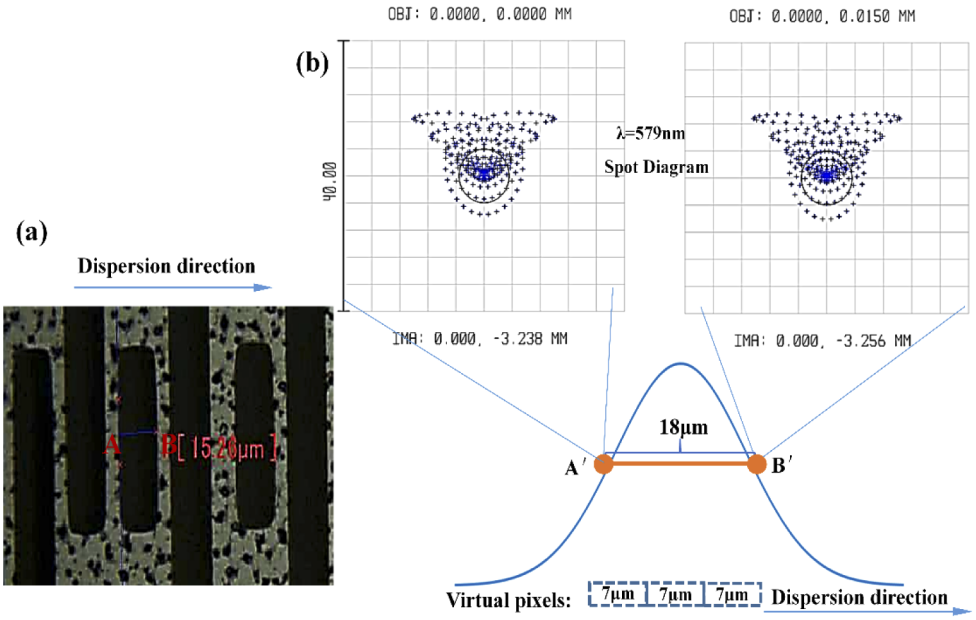

Fig. 7. (a) Measurement of the sub-slit width under the microscope with a large depth-of-field. (b) Simulation calculation of the width of the image of sub-slit on the detector plane.

5. Conclusion

Based on the new micro 2-D slit-array proposed in this article to replace the single slit in typical grating spectrometer, super resolution beyond Nyquist limits can be achieved by the combination of Hadamard transform and sub-pixel reconstruction. In the current work, we used 15th order 2-D slit-array encoded in Hadamard S matrix to generated two kinds of decoded spectra with a half pixel shift from each other, and the FWHM of the reconstructed spectrum is increased to 0.6nm, breaking the experimental system's Nyquist limit of about 0.8nm. This 2-D slit-array adopts an all-solid-state design without any moving parts for better robustness and compactness. Resolution improvement based on this 2-D slit-array hardly affect the spectral detection range of the instrument, and it can achieve real-time spectral detection. The SNR of the instrument is also compensated by the Hadamard transform in the process of super-resolution detection. The usage of this new 2-D slit-array in grating spectrometer shows great potential in the miniaturization of high-performance spectrometers, such as the atomic emission spectrometers.

Funding. National Natural Science Foundation of China (61727813).

Disclosures. The authors declare no conflicts of interest.

References

1. R. Riesenberg, A. Wutting, G. Nitzsche, and B. Harnisch, "Optics MEMS for High-End Micro-Spectrometers," Proc. SPIE **4928**, 6–14 (2002).
2. Z. Yang, T. A. Owen, H. Cui, J. A. Webber, F. Gu, X. Wang, T. C. Wu, M. Zhuge, C. Williams, P. Wang, A. V. Zayats, W. Cai, L. Dai, S. Hofmann, M. Overend, L. Tong, Q. Yang, Z. Sun, and T. Hasan, "Single-nanowire Spectrometers," Science **365**(6457), 1017–1020 (2019).
3. N. Hayazawa, M. Motohashi, Y. Saito, and S. Kawata, "Highly sensitive strain detection in strained silicon by surface-enhanced Raman spectroscopy," Appl. Phys. Lett. **86**(26), 263114 (2005).
4. P. Cheben, J. H. Schmid, A. Delâge, A. Densmore, S. Janz, B. Lamontagne, J. Lapointe, E. Post, P. Waldron, and D. X. Xu, "A high-resolution silicon-on-insulator arrayed waveguide grating microspectrometer with sub-micrometer aperture waveguides," Opt. Express **15**(5), 2299–2306 (2007).

Optics EXPRESS

5. F. G. Peternella, T. Esselink, B. Dorsman, P. Harmsma, R. C. Horsten, T. Zuidwijk, H. P. Urbach, and A. L. C. Adam, "On-chip interrogator based on Fourier transform spectroscopy," Opt. Express **27**(11), 15456–15473 (2019).
6. M. J. E. Golay, "Multi-slit spectrometry," J. Opt. Soc. Am. **39**(6), 437–444 (1949).
7. M. E. Gehm, S. T. McCain, N. P. Pitsianis, D. J. Brady, P. Potuluri, and M. E. Sullivan, "Static two-dimensional aperture coding for multimodal multiplex spectroscopy," Appl. Opt. **45**(13), 2965–2974 (2006).
8. M. Chi, Y. Wu, F. Qian, P. Hao, W. Zhou, and Y. Liu, "Signal-to-noise ratio enhancement of a Hadamard transform spectrometer using a two-dimensional slit-array," Appl. Opt. **56**(25), 7188–7193 (2017).
9. T. Hirschfeld, "Upper boundaries to the extent of the Jacquinot or throughput advantage in Fourier transform infrared spectroscopy," Appl. Spectrosc. **31**(5), 471–472 (1977).
10. C. E. Shannon, "Communication in the presence of noise," Proc. IRE **37**(1), 10–21 (1949).
11. T. Chen, P. B. Catrysse, A. E. Gamal, and B. A. Wandell, "How small should pixel size be?" Proc. SPIE **3965**, 451–459 (2000).
12. P. A. Jansson, *Deconvolution with applications in spectroscopy* (Academic, 1984).
13. L. Xu, H. Yang, K. Chen, Q. Tan, Q. He, and G. Jin, "Resolution enhancement by combination of subpixel and deconvolution in miniature spectrometer," Appl. Opt. **46**(16), 3210–3214 (2007).
14. S. C. Park, M. K. Park, and M. G. Kang, "Super-Resolution Image Reconstruction: A Technical Overview," IEEE Signal Process. Mag. **20**(3), 21–36 (2003).
15. C. Pernechele, L. Poletto, P. Nicolosi, and G. Naletto, "Spectral resolution improvement technique for a spectrograph mounting a discrete array detector," Opt. Eng. **35**(5), 1503–1510 (1996).
16. A. Wuttig, R. Riesenberg, and G. Nitzsche, "Sub-pixel analysis of a double array grating spectrometer," Proc. SPIE **4480**, 334–344 (2002).
17. L. V. Amitonova and J. F. de Boer, "Endo-microscopy beyond the Abbe and Nyquist limits," Light: Sci. Appl. **9**(1), 81 (2020).
18. W. Lukosz, "Optical Systems with resolving powers exceeding the classical limit," J. Opt. Soc. Am. **56**(11), 1463–1471 (1966).
19. T. Konishi, Y. Yamasaki, and T. Nagashima, "Super spectral resolution beyond pixel Nyquist limits on multi-channel spectrometer," Opt. Express **24**(23), 26583–26598 (2016).
20. M. Harwit and N. J. A. Sloane, *Hadamard Transform Optics* (Academic, 1979).
21. T.S. Huang, *Image Sequence Analysis*, (Springer, 1981).
22. G. Nitzsche and R. Riesenberg, "Noise, Fluctuation and Hadamard-Transform-Spectrometer," Proc. SPIE **5111**, 273–282 (2003).
23. P. Hao, M. Chi, and Y. Wu, "Analysis on the optical aberration effect on spectral resolution of coded aperture spectroscopy," Proc. SPIE **10461**, 104610B (2017).
24. L. Zhang, H. Zhang, S. Zhang, and Y. Xue, "Multi-frame Image Super-resolution Reconstruction based on GPOF Registration and L1-norm," in *Sixth International Conference on Natural Computation (ICNC)*, 10–12 (2010).
25. J. M. Bioucas-Dias and M. A. T. Figueiredo, "A new twist: Two-step iterative shrinkage/thresholding algorithms for image restoration," IEEE Trans. on Image Process. **16**(12), 2992–3004 (2007).
26. S. T. McCain, "Coded spectroscopy for ethanol detection in diffuse, fluorescent media," Ph.D. thesis, Duke University (2007).
27. M. Hashimoto and S. Kawata, "Multichannel Fourier-transform infrared spectrometer," Appl. Opt. **31**(28), 6096–6101 (1992).